ELSEVIER

Journal of Alloys and Compounds 452 (2008) 11–15

Journal of ALLOYS AND COMPOUNDS

www.elsevier.com/locate/jallcom

High temperature corrosion of superalloys in a molten salt under an oxidizing atmosphere

Soo-Haeng Cho, Jin-Mok Hur*, Chung-Seok Seo, Seong-Won Park

Korea Atomic Energy Research Institute, 305-353 Daejeon, Republic of Korea

Received 18 September 2006; received in revised form 21 December 2006; accepted 15 January 2007
Available online 17 February 2007

Abstract

The electrolytic reduction of spent oxide fuel involves the liberation of oxygen in a molten LiCl electrolyte, which results in a chemically aggressive environment that is too corrosive for typical structural materials. So, it is essential to choose the optimum material for the process equipment for handling a molten salt. In this study, corrosion behavior of Inconel 713LC, Nimonic 80A and Nimonic 90 in a molten LiCl–Li_2O salt under an oxidizing atmosphere was investigated at 675 °C for 72–216 h. Inconel 713LC alloy showed the highest corrosion resistance among the examined alloys. Corrosion products of Inconel 713LC were Cr_2O_3, $NiCr_2O_4$, Ni and NiO, and those of Nimonic 80A were Cr_2O_3, $LiFeO_2$, $(Cr, Ti)_2O_3$ and $Li_2Ni_8O_{10}$ while Cr_2O_3, $(Cr, Ti)_2O_3$, $LiAlO_2$ and $CoCr_2O_4$ were produced from Nimonic 90. Inconel 713LC showed a local corrosion behavior and Nimonic 80A, Nimonic 90 showed a uniform corrosion behavior.

Keywords: Corrosion behavior; Hot corrosion; Lithium molten salt

1. Introduction

The molten salt technology has been widely applied in the industrial world because of its physical and chemical characteristics, especially its high electrical conductivity, high processing rate, and high diffusion rate. And recently, it has attracted much attention in the fields of jet engines, fuel cells, catalysts, and metal refinement. Therefore, the studies on the corrosion of the structural materials for handling high temperature molten salts have also been continuously carried out. For example, the corrosion of a gas turbine by a molten Na_2SO_4 [1–3] and the corrosion related to a molten carbonate fuel cell [4,5] have been extensively investigated. Also there are many reports on an accelerated oxidation in chloride molten salts [6,7]. However, they are mainly short time electrochemical experiments and few reports are found on long term experiments for the corrosion of commercial alloys in a chloride molten salt by considering the corrosion products, rate and behaviors.

The electrochemical reduction process for spent oxide nuclear fuel is carried out in a LiCl–Li_2O molten salt at 650 °C. The liberation of oxygen on an anode and the high temperature molten salts of the process cause a chemically aggressive environment that is too corrosive for ordinary structural materials. Therefore, for an implementation of the electrochemical reduction technology, corrosion resistance materials should be developed. Guided by the past experience of the Korea Atomic Research Institute, we selected Inconel 713LC, Nimonic 80A, and Nimonic 90 as candidate materials for service in the electrochemical reduction process and investigated their corrosion behaviors under simulated electrochemical reduction conditions.

2. Experimental

The chemical compositions of the used superalloys are shown in Table 1. After the specimens were heated at 1050 °C for 1 h and water cooled to remove an inner defect, they were prepared with dimensions of 70 mm × 15 mm × 2 mm and stabilized at 950 °C for 1 h. Before the corrosion test, the specimens were ground with SiC paper, polished with diamond paste and cleaned in de-ionized water and acetone.

The experimental apparatus is shown in Fig. 1. A LiCl–Li_2O molten salt was introduced into a high-density MgO crucible and then heated at 300 °C for 3 h in an argon atmosphere to remove any possible moisture. After reaching the set conditions, the specimens and alumina tube were immersed into the molten salt, and mixed gas (Ar–10% O_2) was supplied through an alumina tube. The corrosion tests were carried out at 675 °C and for 72–216 h. The Li_2O

* Corresponding author. Tel.: +82 42 868 2028; fax: +82 42 868 4851.
E-mail address: jmhur@kaeri.re.kr (J.-M. Hur).

0925-8388/$ – see front matter © 2007 Elsevier B.V. All rights reserved.
doi:10.1016/j.jallcom.2007.01.169

Table 1
Chemical compositions of tested alloys (wt.%)

Alloy	Ni	Cr	Fe	Co	C	Al	Ti	Nb	Mo
Inconel 713LC	74.00	11.57	0.10	0.08	0.05	6.05	0.76	1.95	4.15
Nimonic 80A	74.90	19.24	1.14	–	0.06	1.68	2.40	–	–
Nimonic 90	59.88	19.38	0.57	16.05	0.058	1.38	2.40	–	–

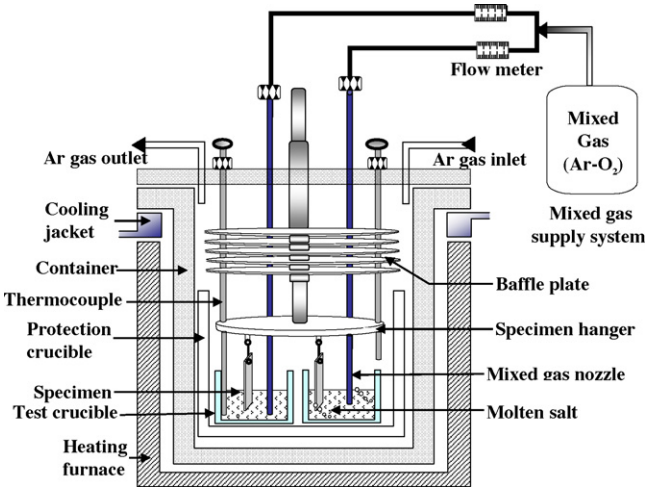

Fig. 1. Schematic diagram of the apparatus for the corrosion test.

concentration in LiCl was 3 wt.%. Following the corrosion test, the specimens were withdrawn from the salt and kept under argon gas while the furnace was cooled to room temperature. The vessel was opened and the specimens removed for a visual examination before a cleaning. The specimens were then cleaned ultrasonically in de-ionized water, measured, and weighed. The corrosion products and fine structures of the corroded samples were analyzed by XRD (X-ray Diffractometer, Rigaku, DMAX/1200), SEM (Scanning Electron Microscope, JEOL, JSM-6300), and EDS (Energy Dispersive X-ray Spectroscope, JEOL, JSM-6300).

3. Results and discussion

3.1. Corrosion rate

The weight loss of the specimens after the corrosion tests in a LiCl–Li_2O molten salt for 72 and 216 h are shown in Fig. 2. Every tested specimen showed a weight loss with time and the corrosion rate was as such: Inconel 713LC < Nimonic 80A < Nimonic 90. 713LC alloy showed the highest corrosion resistance among the examined alloys. The area change and depth of attack for the specimens tested after a 9-day test at 675 °C were investigated and shown in Table 2. In the case of Inconel 713LC, an increase of the cross-sectional area was observed and the reason was attributed to the volume increase due to the formation of corrosion products on the surface. On the other hand, the spallation and the severe progress of corrosion in Nimonic 80A and Nimonic 90 caused the decrease of their cross-sectional area. The relatively shallow depth of attack observed in Inconel 713LC might be attributed to the role of the surface corrosion layer as a protective layer resulting in the suppression of the internal intrusion of a corrosion medium. Considering the corrosion rate measurements shown in Fig. 2, the direction proportion between corrosion rate and depth of attack was identified. The reason for the weight loss of the specimens with time was attributed to a cracking of the protective layer leading to its spallation from the base metal surface. Therefore it was thought that the weight variation of the specimens would be greatly influenced by the adherence between a corrosion layer and a base metal and the stability of a corrosion layer growth.

Table 2
Corrosion results of a 9-day test at 675 °C

Alloy	Cross-sectional area			Depth of attack (μm)
	Initial cross-section area (mm^2)	Post-test area (mm^2)	Area change (mm^2)	
Inconel 713LC	46.184	47.336	+1.152	105.4
Nimonic 80A	46.933	46.864	−0.069	227.1
Nimonic 90	47.297	47.221	−0.076	244.0

3.2. Corrosion products

Fig. 3 shows the XRD patterns of the corrosion products from the corrosion tests at 675 °C for 72 and 216 h. The identification of the corrosion products was performed by the Joint Committee on Powder Diffraction Standards (JCPDS)-the Powder Diffraction File (PDF). The corrosion products of Inconel 713LC were Cr_2O_3, $NiCr_2O_4$, and NiO for 72 and 216 h (Fig. 3(a)). From a thermodynamic point of view, Cr_2O_3 is the most stable oxide in the Ni–Cr–Fe based alloys [8]. Therefore, for Nimonic 80A, Cr_2O_3 was initially formed as a corrosion product. Also the diffusion of the Fe ion and its reaction with the Li based molten salt led to the formation of $LiFeO_2$. And then for the 216 h

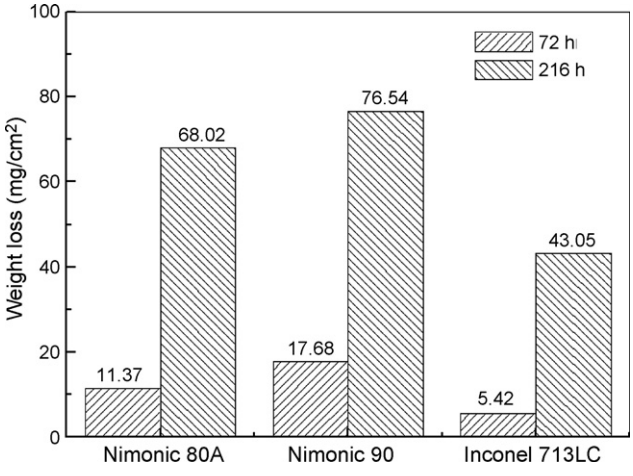

Fig. 2. Weight loss of the alloys corroded at 675 °C, as a function of the time.

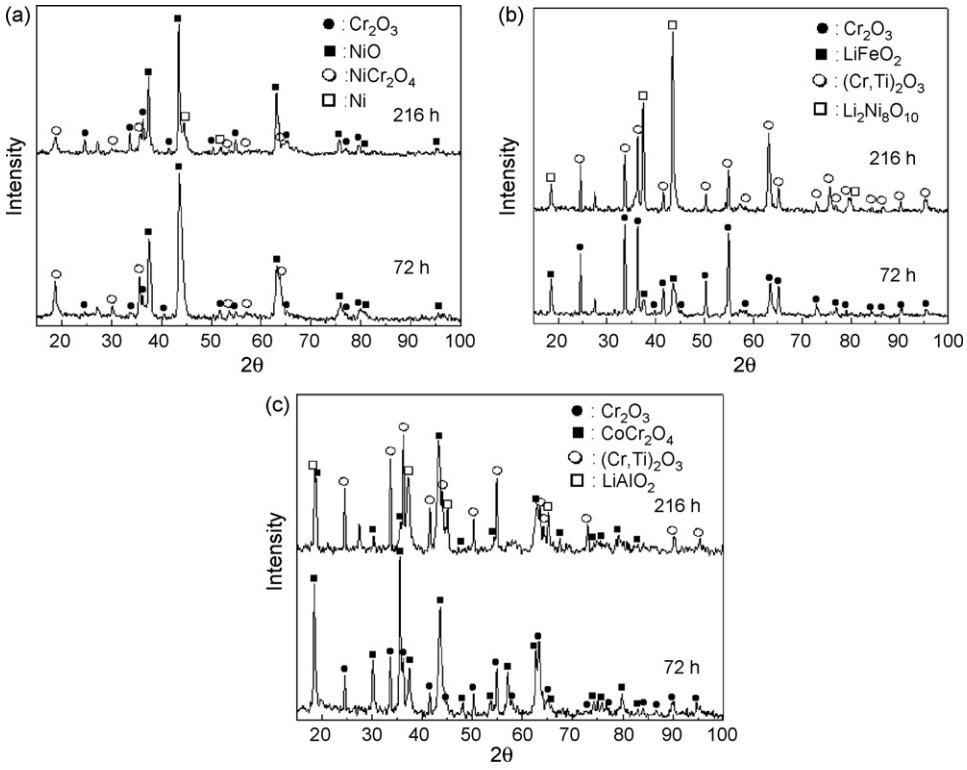

Fig. 3. XRD patterns of the corrosion products of: (a) Inconel 713LC, (b) Nimonic 80A, and (c) Nimonic 90 corroded at 675 °C for 72 and 216 h.

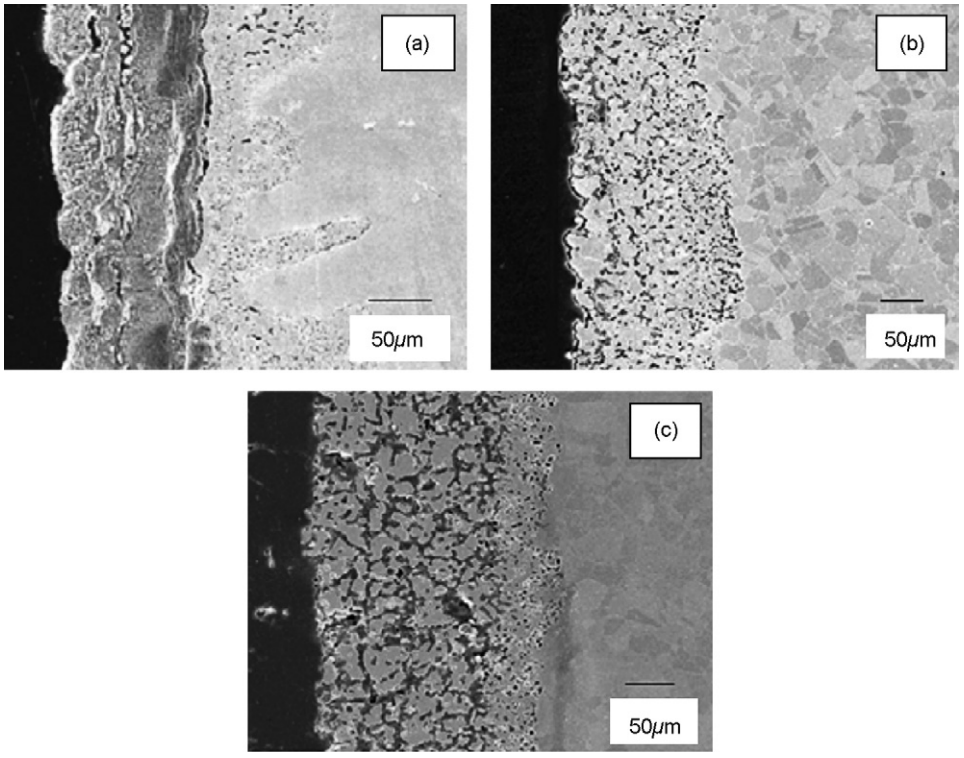

Fig. 4. Cross-sectional SEM images of (a) Inconel 713LC, (b) Nimonic 80A and (c) Nimonic 90 corroded at 675 °C for 216 h.

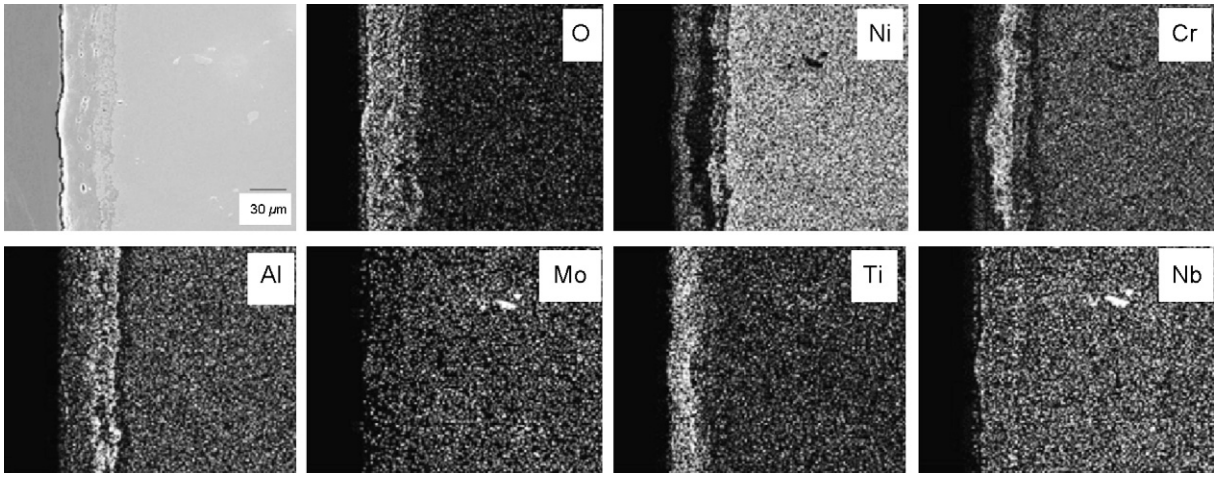

Fig. 5. Cross-sectional SEM image and elemental distribution of Inconel 713LC corroded at 675 °C for 72 h.

conditions, the formation of $Li_2Ni_8O_{10}$ and $(Cr, Ti)_2O_3$ was observed (Fig. 3(b)). Fig. 3(c) shows that the corrosion products of Nimonic 90 where Cr_2O_3 and $CoCr_2O_4$ for 72 h and $(Cr, Ti)_2O_3$ and $LiAlO_2$ for 216 h, respectively.

3.3. Corrosion behaviors

Fig. 4 shows the SEM images of the specimens corroded for 216 h. Contrary to the corrosion of Inconel 713LC, an outer corrosion layer was not observed for Nimonic 80A and Nimonic 90. Local corrosion behavior for Inconel 713LC and a uniform corrosion behavior for Nimonic 80A and Nimonic 90 were observed, respectively. The content of Cr affected markedly on the uniform corrosion pattern due to the their depletion [9]. The formation of a dense protective corrosion layer of Inconel 713LC (Fig. 4) and its lower corrosion rate have a close correlation.

Cross-sectional SEM image and elemental maps of Inconel 713LC corroded for 72 h are shown in Fig. 5. The corrosion layer was dense and adherent. The outer layer mainly consisted of Cr, Ni-oxides. A solid reaction between the surface NiO and Cr_2O_3 might cause the formation of the $NiCr_2O_4$ spinel oxides observed in Fig. 3(a) [10,11]. The oxygen active elements such as Al and Ti were preferentially oxidized and participated in the corrosion layer [8]. It was reported that the addition of 4–5 wt.% Al enhanced the oxidation-resistance of alloys by the formation of an Al_2O_3 protective layer [12]. Ni is an element which inhibits the internal diffusion of an oxygen ion by its accumulation on the interface of oxide/oxide or beneath of the oxide layers [13]. In this study, the enrichment of Ni in an inner corrosion layer was observed and thus Ni was considered as a useful element for the enhancement of the corrosion resistance in a oxidative molten salt.

Fig. 6 shows the cross-sectional SEM image and elemental maps of Nimonic 80A corroded for 72 h. The dense outer layer mainly consisted of Cr, Fe-oxides. The diffusion coefficients of the metal ion in the oxides are in the order of $Fe^{3+} > Fe^{2+} > Ni^{2+} > Cr^{3+}$ [10]. Therefore, the diffusion of the Fe ion through the initially formed Cr_2O_3 layer and its reaction with a molten salt resulted in $LiFeO_2$. The preferential oxidation of Al and Ti beneath the outer corrosion layer and its

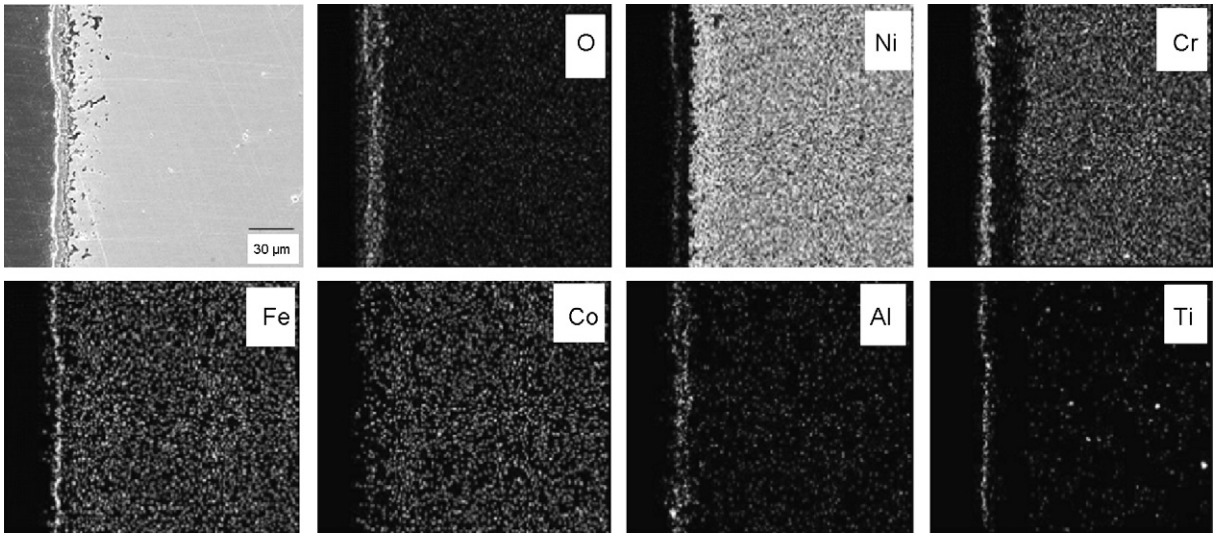

Fig. 6. Cross-sectional SEM image and elemental distribution of Nimonic 80A corroded at 675 °C for 72 h.

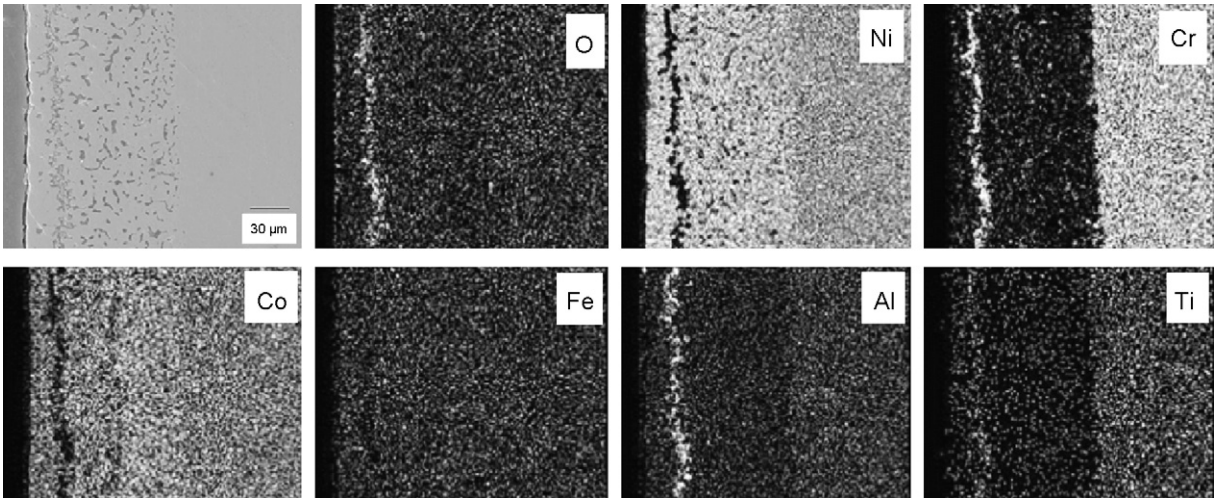

Fig. 7. Cross-sectional SEM image and elemental distribution of Nimonic 90 corroded at 675 °C for 72 h.

participation in the corrosion layer formation were also observed [8].

Cross-sectional SEM image and elemental maps of Nimonic 90 corroded for 72 h are shown in Fig. 7. The outer corrosion layer was spalled and only an inner corrosion layer was observed. It was thought that the solid reactions between the thermodynamically stable oxide, Cr_2O_3 and CoO formed from the preferential oxidation of Co resulted in the formation of the $CoCr_2O_4$ spinel oxides (see also Fig. 3(c)) [10,11]. Fig. 7 also shows the formation of the oxides of Al and Ti beneath the Ni-rich layer. It is suggested that the oxidation of the oxygen active elements occurred after the preferential oxidation of Cr and Co. Wood et al. [11] reported the existence of a Cr depletion region beneath an outer corrosion layer, Cr_2O_3 and the reason was attributed to the consumption of the Cr for an oxide formation. Therefore with the progress of the oxidation, the Cr depletion region would expand into the inside of the alloys because Cr diffuses out from the base metal to supplement the consumed Cr (Fig. 7). The thermal stress by the difference of the thermal expansion coefficients between a base metal and an oxide layer and the growth stress due to an oxide layer growth would cause a spallation of the oxide layers. Therefore, the growth and spallation cycle of the oxide layer will also deplete the Cr element which is a constituent of the corrosion layer.

4. Conclusions

The corrosion behavior of superalloys in a oxidative LiCl–Li_2O molten salt was investigated in association with the electrochemical reduction process. The corrosion rate was in the order of Inconel 713LC < Nimonic 80A < Nimonic 90. Corrosion products of Inconel 713LC were Cr_2O_3, $NiCr_2O_4$, Ni and NiO, and those of Nimonic 80A were Cr_2O_3, $LiFeO_2$, $(Cr, Ti)_2O_3$ and $Li_2Ni_8O_{10}$. Cr_2O_3, $(Cr, Ti)_2O_3$, $LiAlO_2$ and $CoCr_2O_4$ were identified as the corrosion products of Nimonic 90. Inconel 713LC showed a local corrosion behavior while Nimonic 80A, Nimonic 90 showed a uniform corrosion behavior. Ni was concentrated around the inner oxide layers and it retarded the corrosion rate. The high content of Cr caused a growth stress and a depletion of the elements in the corrosion layer. So it was concluded that an excess Cr causes deleterious effects on the corrosion resistance of alloys. Oxygen active elements, such as Al and Ti, enhanced the corrosion resistance by a protective oxide layer formation.

Acknowledgement

This work was funded by the National Mid- and Long-term Atomic Energy R&D Program supported by the Ministry of Science and Technology of Korea.

References

[1] F.J. Kohl, G.J. Santoro, C.A. Stearns, G.C. Fryburg, D.E. Rosner, J. Electrochem. Soc. 126 (1979) 1054–1061.
[2] J.A. Goebel, F.S. Pettit, Met. Trans. 1 (1970) 1943–1954.
[3] F.S. Pettit, J.A. Goebel, G.W. Goward, Corros. Sci. 9 (1969) 903–913.
[4] M. Spiegel, P. Biedenkipf, H.J. Grabke, Corros. Sci. 39 (1997) 1193–1210.
[5] S. Mitsushima, N. Kamiya, K.I. Ota, J. Electrochem. Soc. 137 (1990) 2713–2716.
[6] F. Colom, A. Bodalo, Corros. Sci. 12 (1972) 731–738.
[7] W.H. Smyrl, M.J. Blanckburn, Corrosion 31 (1975) 370–375.
[8] E.T. Turkdogan, Physical Chemistry of High Temperature Technology, Academic Press, New York, 1980.
[9] A. Tahara, T. Shinohara, Corros. Sci. 47 (2005) 2589–2598.
[10] H. Izuta, Y. Komura, J. Jpn. Inst. Met. 58 (1994) 1196–1205.
[11] G.C. Wood, F.H. Stott, Mater. Sci. Technol. 3 (1987) 519–530.
[12] Y. Harada, Jpn. Therm. Spray Soc. 33 (1996) 128–134.
[13] G.C. Wood, B. Chattopadhyay, Corros. Sci. 10 (1970) 471–480.